Chapter 2
Radio Emission Properties of Pulsars

Richard N. Manchester

2.1 Introduction

Pulsars are fascinating objects with a wide range of applications in physics and astronomy. Characterised observationally by a highly periodic pulse train with periodicities typically in the range a few milliseconds to several seconds, they are generally identified with highly magnetised and rapidly rotating neutron stars formed in supernova explosions. Rotation of the star causes beamed emission, probably emanating from open field lines associated with the magnetic poles, to sweep across the sky generating one observed pulse per rotation period. A total of 1,765 pulsars are now known and almost all of these lie within our Galaxy.[1] As Fig. 2.1 illustrates, pulsars come in two main classes, those with periods in the millisecond range and the so-called "normal" pulsars with periods of order 1 s. Most millisecond pulsars (MSPs) are binary, that is, in an orbit with another star, whereas only a few percent of normal pulsars are binary. MSPs, which comprise about 10% of the known population, are believed to be relatively old pulsars which have been spun up or "recycled" by accretion from a binary companion [3]. Because of exchange interactions occurring in their dense cores, globular clusters are a fertile breeding ground for MSPs [10] and about three-quarters of the known MSPs are associated with these clusters.

Pulsar periods are extremely stable but they are not constant. All pulsars are slowing down because of loss of rotational kinetic energy to some combination of magnetic-dipole radiation (electro-magnetic waves at the pulsar spin frequency) and relativistic particle outflow. The spin-down rate can be expressed as

$$\dot{\nu} = -K\nu^n \,, \tag{2.1}$$

R.N. Manchester
Australia Telescope National Facility, CSIRO, P.O. Box 76, Epping, NSW 1710, Australia
e-mail: dick.manchester@csiro.au

[1] Pulsar parameters used in this paper have been obtained from the ATNF Pulsar Catalogue, Version 1.29, http://www.atnf.csiro.au/research/pulsar/psrcat [44].

W. Becker (ed.), *Neutron Stars and Pulsars,* Astrophysics and Space Science Library 357,

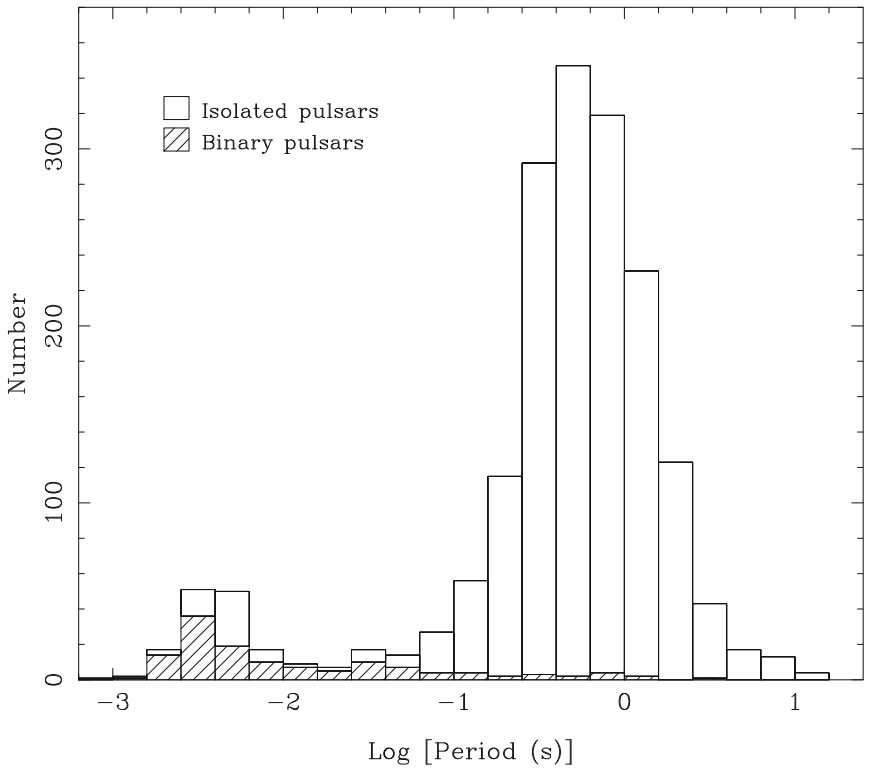

Fig. 2.1 Histogram of observed pulsar periods. Pulsars which are members of a binary system are identified

where K depends on the magnetic field strength at the stellar surface, B_s, and the neutron-star moment of inertia, I, and n is the braking index. For pure magnetic-dipole braking, $n = 3$ and

$$K = \frac{8\pi^2 B_s^2 R^6 \sin^2\alpha}{3Ic^3}\ , \tag{2.2}$$

where α is the inclination angle of the dipole magnetic axis relative to the spin axis.

We can define a "characteristic age" for the pulsar $\tau_c = P/(2\dot{P})$, where $P = 1/\nu$ is the pulsar period and $\dot{P}$ is its first time derivative. If the pulsar was born with a period much less than the present value and its spin-down is characterized by a braking index close to 3.0, then the characteristic age is a good indicator of the true age. We can also estimate the strength of the dipole field at the neutron-star surface, $B_s = 3.2 \times 10^{19}(P\dot{P})^{1/2}$ G, where $n = 3$, $I = 10^{45}$ g cm^2 and $\alpha = 90^\circ$ have been assumed.

Figure 2.2 shows the observed distribution of pulsars on the P–$\dot{P}$ plane. MSPs have very low spin-down rates and hence relatively weak magnetic fields compared to normal pulsars. In contrast, Anomalous X-ray Pulsars (AXPs)[2] lie in the upper

[2] Soft Gamma-ray Repeaters (SGRs) with coherent pulsations are included in the AXP classification.

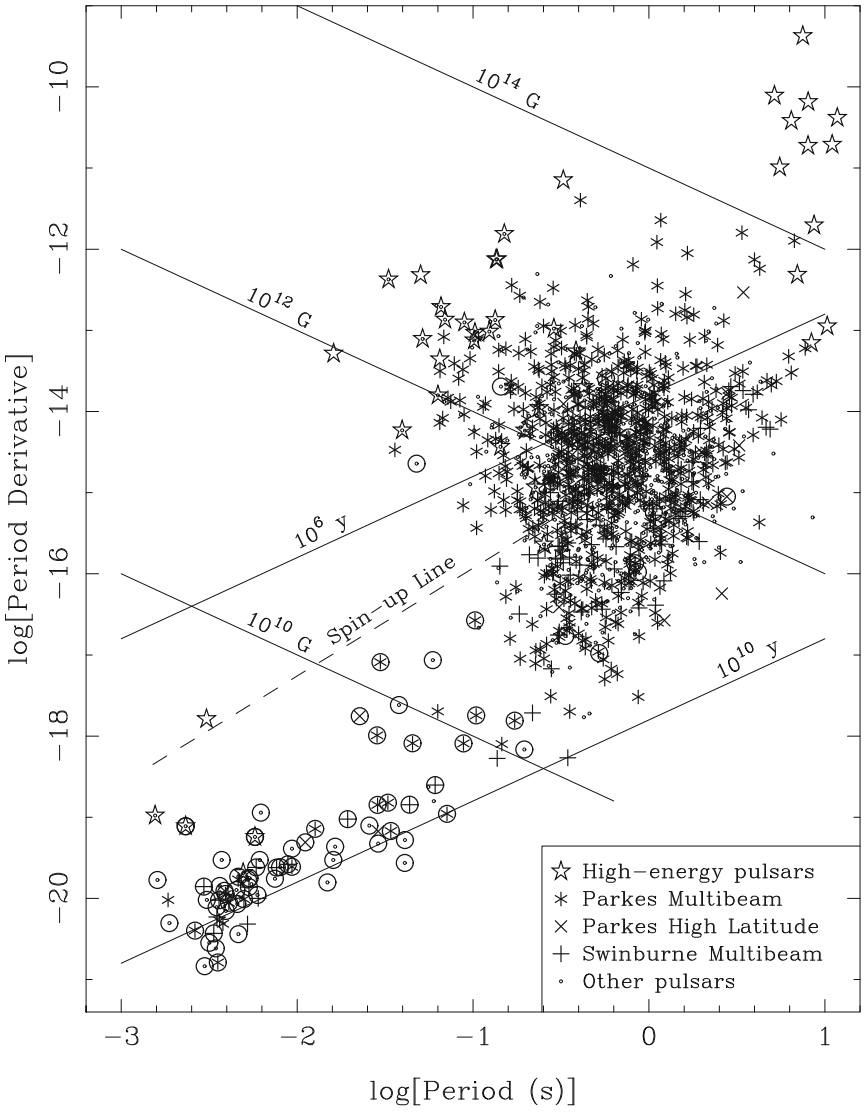

Fig. 2.2 Distribution of pulsars versus pulse period and period derivative. Pulsars which have detectable pulsed emission at high energies (optical, X-ray and γ-ray), including the so-called Anomalous X-ray Pulsars (AXPs), are indicated. Lines of constant characteristic age and surface dipole magnetic field are shown, along with the "spin-up line", the minimum period attainable through accretion from a binary companion. Pulsars discovered in the principal recent pulsar surveys are indicated

right corner of the P–$\dot{P}$ diagram with periods in the range 5–12 s and very strong implied magnetic fields in the range 10^{14}–10^{15} G. Despite their rapid spin-down, the X-ray luminosity of these "magnetars" is too great to be powered by the rotational energy loss; decay of the super-strong magnetic fields is believed to be the energy

source [11]. Young pulsars lie predominantly in the upper left part of the diagram with magnetic fields of order 10^{12} G. For $n = 3$, these pulsars will evolve along lines of constant magnetic field into the region occupied by the bulk of the known pulsar population. Lying between the MSPs and the tail of the normal pulsar distribution, there is an important group of group of binary pulsars. These systems are characterized by relatively massive companions and include all of the known double-neutron-star systems. Because of the rapid evolution of the binary companion, the recycling phase was relatively short-lived in these systems and so these pulsars typically have intermediate periods in the range 20–100 ms.

More than half of the known pulsars have been discovered in the past few years, most notably using the 20-cm multi-beam receiver on the Parkes 64-m radio telescope in NSW, Australia. The main surveys undertaken with this system are described in Sect. 2.2 and other recent surveys using the 300-m Arecibo radio telescope and the 100-m Green Bank Telescope are described in Sect. 2.3. In the remainder of the review, some interesting recent results related to the pulsar emission mechanism are described – no claim to completeness is made. Recent results on pulse nulling and mode changing are described in Sect. 2.4. Recent results on pulse-to-pulse modulations and subpulse drifting are discussed in Sects. 2.5 and 2.6 describes recent observations of "giant" pulses and their implications. The extraordinary detection of transient radio emission from the magnetar XTE J1810-197 (PSR J1809−1943) is described in Sect. 2.7. Some recent results on the polarisation of young pulsars are described in Sect. 2.8. Some concluding remarks are given in Sect. 2.9.

2.2 Parkes Multi-Beam Pulsar Surveys

The Parkes 20-cm multi-beam receiver has 13 beams arranged in a double hexagon around a central beam and operates at a central frequency of 1,374 MHz [59]. The beams are spaced by two beam-widths on the sky but, by combining sets of four pointings, a given region of sky can be completely covered with beams overlapping at the half-power points. Each beam has two probes receiving orthogonal linear polarizations and, after amplification and down-conversion, each of the 26 signals is fed to a 96×3 MHz filterbank giving a total bandwidth of 288 MHz. Signals from corresponding polarizations are then detected, summed, high-pass filtered, one-bit digitized and recorded to magnetic tape for subsequent analysis.

A number of very successful pulsar surveys have been undertaken with this instrument. The most prolific is the Parkes Multibeam Pulsar Survey [45] which covered a 10°-wide strip along the southern Galactic plane from $l = 260°$ to $l = 50°$ using a sampling interval of 250 μs. The observation time per pointing was relatively long, 35 min, and so the survey was quite sensitive with a limiting flux density of approximately 0.2 mJy for longer-period pulsars unaffected by dispersion smearing within a filter channel. A total of 3,080 pointings was required to cover the survey area. Survey observations commenced in mid-1997 and were completed in 2003.

The data were processed on work-station clusters at ATNF, Jodrell Bank Observatory and McGill University resulting in the detection of 1,015 pulsars of which 760 were new discoveries. Following confirmation of each pulsar, at least 18 months of timing observations were carried out in order to obtain accurate astrometric and timing parameters (cf. Fig. 2.2). A series of papers [16, 23, 34, 38, 45, 49] gives details of all of the pulsars detected and discusses various implications of the results. For example, Kramer et al. [34] discuss the properties of young pulsars and show that about 20 of the known pulsar population are likely to be associated with currently unidentified gamma-ray sources.

The Parkes Multibeam Pulsar Survey database was also searched for isolated dispersed pulses, leading to the discovery of an apparently new class of pulsars, the so-called Rotating Radio Transients or RRATs. McLaughlin et al. [46] detected eleven of these objects which emit an individual strong pulse at intervals ranging from minutes to hours. Careful analysis of the pulse arrival times led to the identification of underlying periodicities in the range 0.4–6 s and, in three cases, to a full timing solution showing the steady period increase typical of pulsars. There is little doubt that RRATs are rotating neutron stars but considerable doubt as to whether they are normal, albeit highly modulated, pulsars near the end of their active life [68] or a distinct population with different birth properties.

A companion survey to the Parkes Multibeam Pulsar Survey, the Parkes High-Latitude Pulsar Survey, was carried out by the same group [5]. This survey covered the region $|b| < 60^\circ$, $220^\circ < l < 260^\circ$ with a shorter sampling interval, 125 μs, and observation time, 4 min, to optimize sensitivity to MSPs and binary pulsars. Data processing for this survey was carried out on clusters at Bologna Astronomical Observatory, Cagliari Astronomical Observatory and Jodrell Bank Observatory. A total of 42 pulsars was detected and 18 of these were new discoveries. Four of the new discoveries are MSPs and three of these four are binary. They include the famous "double pulsar" PSR J0737−3039A/B, the first-known binary pulsar in which both stars are detectable as pulsars [4, 40].

Lorimer et al. [38] discuss the properties of the Galactic population of pulsars based on the results of these two surveys. Figure 2.3 shows the observed and derived distributions in Galactocentric radius and Galactic z-distance, and the derived luminosity function and initial period distribution along with fitted functions to these distributions for two different assumed distributions for the free electrons in the Galaxy – see Lorimer et al. [38] for details of the procedures and the fitted functions.

It is clear that the derived radial distributions (Fig. 2.3a) are strongly dependent on the assumed distribution of free electrons. In particular, the existence of a deficit in the population near the Galactic Centre is quite uncertain, depending entirely on the poorly known electron distribution in the central region. Integration of the derived radial distributions gives a total Galactic population of about 30,000 potentially detectable pulsars with luminosity above 0.1 mJy kpc^2. Assuming that pulsar emission is beamed according to the function derived by Tauris and Manchester [62], the total number of pulsars in the Galaxy with luminosity above 0.1 mJy kpc^2 is derived to be $148,000 \pm 6,000$ for the azimuthally symmetric Model S [41] and $155,000 \pm 6,000$ for the "clumpy" Model C [8].

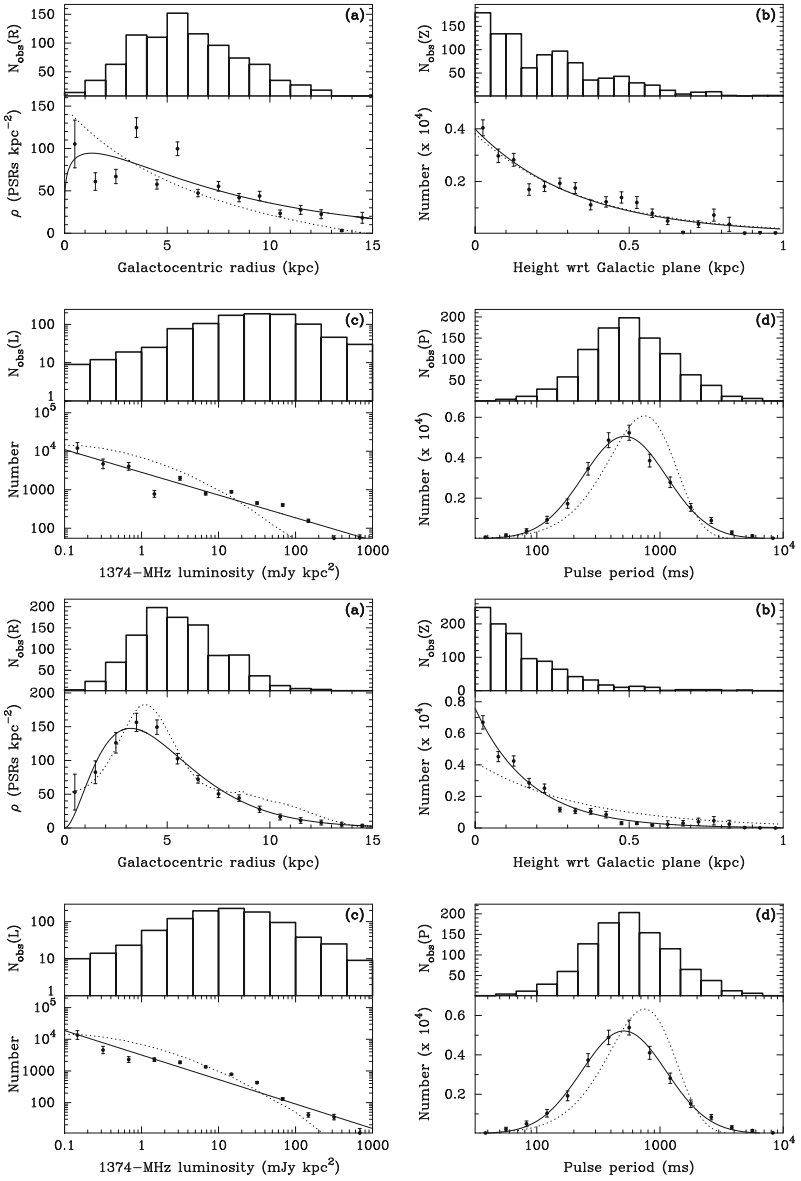

Fig. 2.3 Observed distributions in Galactocentric radius (**a**) and Galactic z-distance (**b**) from the Parkes Multibeam Pulsar Survey data (*upper panels*) and derived distributions for the Galactic pulsar population taking into account survey selection effects (*lower panels*). The *solid lines* are a fit of suitable functions to the derived distributions. The observed and derived luminosity functions are shown in plot (**c**) and the distributions of initial (birth) spin period are given in plot (**d**). Two models for the Galactic free electron distribution are considered, the azimuthally symmetric model of Lyne, Manchester and Taylor [41] (Model S, upper group of four plots) and that of Cordes and Lazio [8] (Model C, lower group of four plots). The *dotted curves* show (**a**) the assumed free electron distribution, (**b**) an exponential distribution of scale height 350 pc, (**c**) the log-normal luminosity function derived by Faucher-Giguère and Kaspi [15] and (**d**) an initial-period distribution used by Kolonko et al. [32]

The derived z distributions are also very dependent on the assumed electron density distributions, with a scale height of about 330 pc for Model S and 180 pc for Model C. Independent studies of the z distribution [47] and the observed distribution of pulsars detected in the Parkes High-Latitude Pulsar Survey [5] are more consistent with the larger scale height.

The derived luminosity function is well fitted by a simple power law but its slope of -0.6 (Model S) or -0.8 (Model C) is flatter than that obtained from earlier studies. The derived initial period distribution is well fitted by a log-normal distribution peaking at about 500 ms. A pulsar current analysis gives a birthrate of 0.34 ± 0.05 per century for potentially detectable pulsars with luminosity greater than 0.1 mJy kpc^2 in the Galaxy. With beaming taken into account, the derived birthrate is approximately 1.3 pulsars per century, depending on the beaming model assumed.

A group based at Swinburne University of Technology used the Parkes multibeam system to search Galactic latitudes between 5° and 30° with the same longitude range as the Parkes Multibeam Pulsar Survey. Like the Parkes High-Latitude Pulsar Survey, the Swinburne survey used a faster sampling interval and shorter observation time to give improved sensitivity for millisecond and binary pulsars [13,25]. The survey detected 230 pulsars of which 95 were new discoveries. Notable amongst them was PSR J1909−3744 , a 2.5-ms pulsar in a 1.5-day orbit with a very narrow pulse, only 42 μs wide at the half-power point [26]. This leads to very precise pulse timing which has enabled an accurate parallax measurement (implied distance 1.14 ± 0.04 kpc) and an accurate measurement of the Shapiro delay, leading to a value for the pulsar mass of $1.438 \pm 0.024\ M_\odot$ [27].

Another recent survey undertaken with the Parkes multi-beam receiver is a deep search for pulsars in the Magellanic Clouds [43]. Observation times were 2.3 h per pointing giving a limiting mean flux density for isolated or long-period binary pulsars of 0.12 mJy. The survey required 73 pointings for the Small Magellanic Cloud and 136 pointings for the Large Magellanic Cloud. A total of 14 pulsars was discovered, 12 of which are believed to lie in the Magellanic Clouds. These discoveries bring the total number of pulsars known in the Clouds to 20. Only the high end of the luminosity function is sampled, but the derived values are consistent with the luminosity function for Galactic pulsars. Although the sample is relatively small, there was no evidence for a significant dependence of radio luminosity on either pulsar period or characteristic age.

2.3 Other Recent Surveys

Initial results from a pulsar survey using the Arecibo L-band Feed Array (ALFA) system have been reported by Cordes et al. [7]. The ALFA system has seven beams with a bandwidth of 300 MHz centred on 1,375 MHz. Currently the Pulsar ALFA (PALFA) survey is using signal processors of bandwidth 100 MHz but ultimately the full 300 MHz bandwidth will be used. The PALFA survey plans to

cover $|b| < 5^\circ$ for the two regions of the Galactic plane accessible to the Arecibo telescope, $40^\circ < l < 75^\circ$ and $170^\circ < l < 210^\circ$, but the current observations are restricted to $|b| < 1^\circ$. The observation time per pointing is 134 s for the first region, giving a limiting flux density for long-period, low-DM pulsars of about 0.07 mJy, and 67 s for the anti-centre region with a correspondingly reduced sensitivity. From a preliminary analysis of the data, 11 previously unknown pulsars have been discovered and 29 previously known pulsars detected. One of the new discoveries, PSR J1906+0746, is a relatively young pulsar with a pulse period of 144 ms in a mildly eccentric ($e = 0.085$) 3.98-h orbit [39]. Relativistic perturbations to the orbit are detectable; specifically a periastron advance of $7^\circ.57 \pm 0^\circ.03\,\mathrm{yr}^{-1}$ has been observed, implying a total system mass of $2.61 \pm 0.02\,\mathrm{M}_\odot$. It is not clear if the companion is a heavy white dwarf (with the system having a similar evolutionary history to PSR J1141−6545) or a second neutron star. Another of the new discoveries, PSR J0628+09, is an extremely sporadic emitter with a period of 1.2 s that was discovered in a single-pulse search but not detected in the standard periodicity search. Cordes et al. [7] predict that the PALFA survey will ultimately discover about 1,000 pulsars, but Lorimer et al. [38] suggest a smaller number, about 375 new discoveries.

An outstandingly successful search for pulsars in the globular cluster Terzan 5 using the 100-m Green Bank Telescope has been undertaken by Ransom et al. [53]. Observations during 2004 using a receiving system with 600 MHz of bandwidth centred on 1,950 MHz with a sampling interval of about 80 μs were analysed to reveal a total of 21 previously unknown pulsars in the cluster, bringing the total known to 24 (Fig. 2.4). All of the new pulsars appear to be recycled, but their

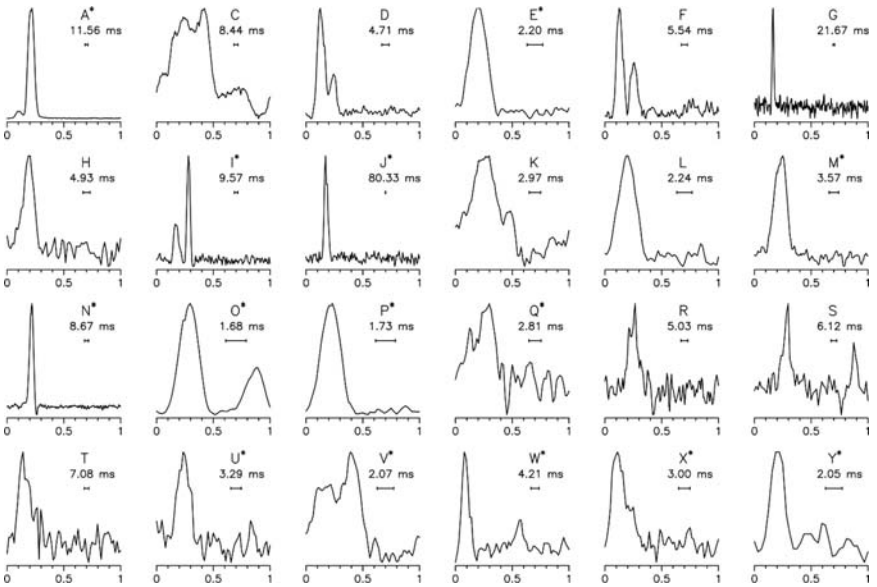

Fig. 2.4 Pulse profiles recorded at the Green Bank Telescope for 24 pulsars in the globular cluster Terzan 5 [53]. The central observing frequency was 1,950 MHz. For each profile the pulsar period and extent of profile smearing (∼0.3 ms) are indicated. An *asterisk* indicates that the pulsar is a member of a binary system

periods cover a larger range, 1.6–80 ms, than the pulsars associated with 47 Tucanae. Thirteen of the new pulsars are binary, with orbital periods in the range 0.25–60 days and near-circular orbits except for two, PSR J1748−2446I and PSRJ 1748−2446J. These two systems respectively have orbital periods of 1.3 and 1.1 days, eccentricities of 0.43 and 0.35 and companion masses greater than 0.24 $M_\odot$ and 0.38 $M_\odot$. With these parameters, relativistic orbit perturbations are detectable. The observed periastron advance leads to total masses of close to $2.2M_\odot$ for both systems, implying most probable pulsar masses of about $1.7M_\odot$, much higher than accurately measured pulsar masses in other pulsar binary systems.

Continued observations and data analysis have led to the discovery of even more pulsars in this cluster. Although details of these further results (with one exception) are not yet formally published, the compilation by Paulo Freire at http://www.naic.edu/ pfreire/GCpsr.html lists a total of 33 pulsars associated with Terzan 5. This one cluster therefore contains about 25% of the total known cluster pulsar population and nearly 20% of all known MSPs! Most notable of the recent discoveries is PSR J1748−2446ad which has the shortest period of any known pulsar, 1.396 ms, corresponding to a spin frequency of 716 Hz [21]. The pulsar is binary in a circular orbit of period 1.04 days and with a companion of minimum mass 0.14 $M_\odot$. As with several other pulsars in short-period binary systems in the cluster, the pulsar is eclipsed for about 40% of the orbit, presumably by an ablated wind from the companion. The mean pulse profile has a weak interpulse approximately midway between the main pulses and its mean flux density at 1,950 MHz is only 80 μJy.

2.4 Pulsar Nulling and Mode Changing

Pulsar nulling is a phenomenon observed mostly in longer-period pulsars in which the pulsed emission abruptly turns off for intervals which range from a few pulse periods to many weeks in different pulsars and then just as abruptly turns on. Mode changing is an apparently related phenomenon in which the mean pulse profile abruptly changes to a different form and then, typically a few minutes later, reverts to the original form. Other pulse properties such as polarisation, subpulse drifting and pulse microstructure are affected by these transitions, showing that they represent a fundamental change in the emission process.

With its relatively long observation time per pointing, the Parkes Multibeam Pulsar Survey provided an excellent database for studies of these phenomena. Wang et al. [65] studied 23 pulsars for which the survey observations showed evidence for nulling behaviour. Figure 2.5 shows a selection of these illustrating the range of "null fraction", i.e., fraction of time that a pulsar spends in the null state. Seven of the 23 pulsars have null fractions in excess of 40% and, with just one short burst during a 2-h observation, PSR J1717−4054 has the largest observed null fraction, >95%.

The close relationship between nulling and mode changing is illustrated by the fascinating behaviour of PSR J1326−6700 shown in Fig. 2.6. The normal emission

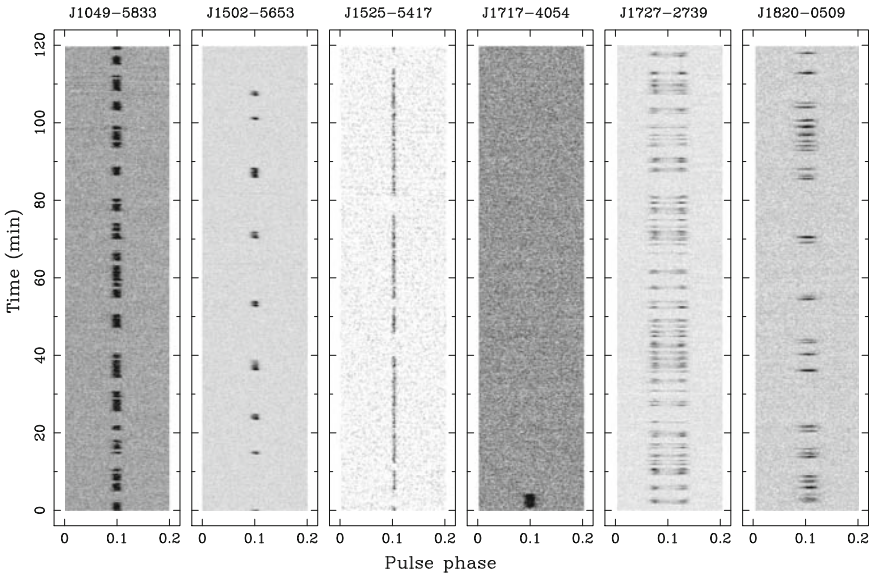

Fig. 2.5 Phase–time plots for six pulsars showing nulling behaviour [65]. A wide range on null fractions and timescales is represented by these examples

from this pulsar has a broad pulse profile with three main components. Every few minutes it switches to a different mode in which essentially all of the normal emission ceases and a new pulse component appears at the leading edge of the normal-mode profile. Another demonstration of the close relationship between nulling and mode changing is provided by PSR B0826−34. This long-period (1.848 s) pulsar is characterized by a very wide pulse profile covering essentially the whole pulse period, complicated drifting subpulse behaviour and very extended null intervals [12]. The null fraction is at least 70% and observed null intervals range in length from a few pulse periods to many hours. Recent observations using the Parkes radio telescope at 1,374 MHz by Esamdin et al. [14] show that the pulsar does not turn off completely in the "null" intervals. Integration of the "null" data show a weak pulse of mean flux density about 2% of that in the "on" phase. As shown in Fig. 2.7, the mean pulse profile in the "null" phase is quite different to that in the "on" phase, showing that the apparent nulls are actually mode changes. Nulls are just an absence of detectable emission and the limits on emission in the null intervals vary, but are at best about 1% of the on-phase flux density. It is possible that, with sufficient sensitivity, pulsed emission would always be found in so-called null intervals. It is clear that both nulls and mode changes result from a large-scale and persistent changes in the magnetospheric current distribution which result in a dramatic change in the radiated beam. Whether it is called a null or a mode change just depends on whether or not a significant part of the modified beam crosses the Earth.

Another interesting recent result which has implications for the interpretation of pulse nulling is the detection of a change in the rate of spin-down during the

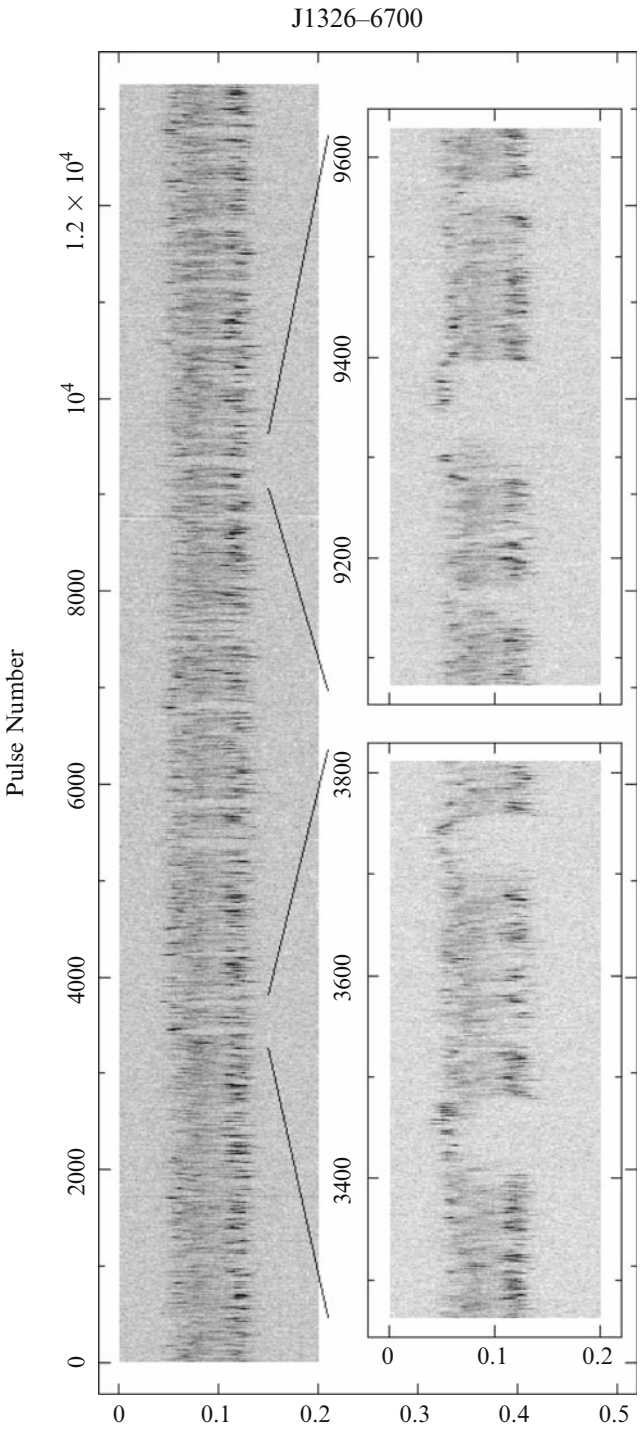

Fig. 2.6 Phase–time plot for individual pulses from PSR J1326−6700. The total data span is a little over 2 h. The *insets* show two portions of the dataset with an expanded scale [65]

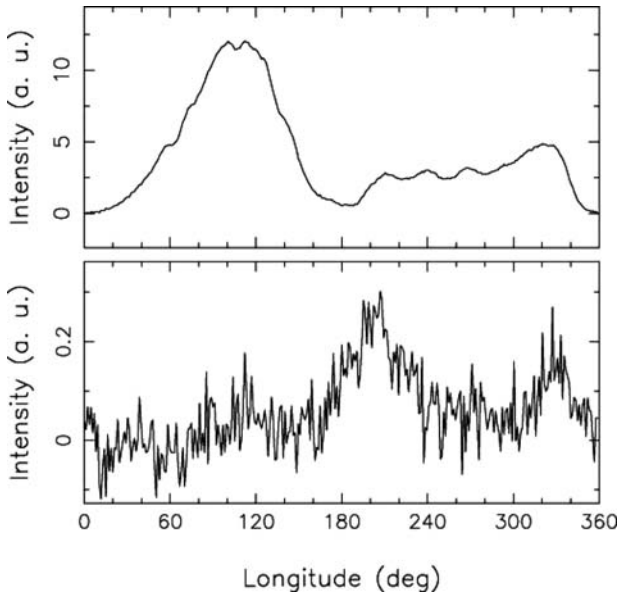

Fig. 2.7 Mean pulse profiles for PSR B0826−34 in its "on" phase (*upper*) and "off" phase (*lower*) [14]

null phase for PSR B1931+24 [35]. This pulsar has a quasi-periodic modulation in which the pulsar is on for 5–10 days and then undetectable for 25–35 days. Because of this long timescale it is possible to measure $\dot{\nu}$ for each "on" phase and compare that with the long-term $\dot{\nu}$. Figure 2.8 illustrates the fascinating result that when the pulsar is on, the spin-down rate $\dot{\nu} = (-16.3 \pm 0.4) \times 10^{-15}\,\mathrm{Hz\,s^{-1}}$, about 50% greater than the value in the off state, $(-10.8 \pm 0.2) \times 10^{-15}\,\mathrm{Hz\,s^{-1}}$, derived from a fit to the timing residuals. This result clearly demonstrates that the magnetospheric currents responsible for the emission of the radio beam also contribute to the pulsar braking. Remarkably, if it is assumed that the braking in the null state is solely due to magnetic-dipole radiation and that the magnetospheric currents are zero in this state, then the magnetospheric charge density in the on state required to generate the additional braking is almost exactly equal to the Goldreich–Julian value [17].

The implication that magnetospheric currents completely switch off in the null state appears somewhat at odds with our previous conclusion that nulls are basically mode changes where the radio beam is either much weaker than in the on state or is redirected so that it doesn't sweep over the Earth as the pulsar rotates. However, it is quite possible that in a null-like mode change either the magnitude of the current or its effectiveness in braking the pulsar is significantly reduced, but not necessarily zero. This leaves open the fractional contribution of magnetic-dipole radiation to the braking and implies magnetospheric charge densities greater than the Goldreich–Julian value, at least in the on state.

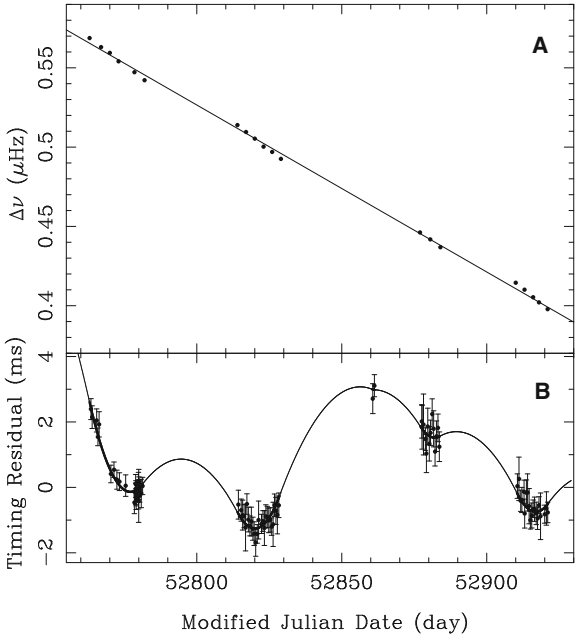

Fig. 2.8 Long-term timing behaviour of the nulling pulsar PSR B1931+24. *Panel-A* gives the time variation of pulse frequency, showing that the spin-down rate is larger than average when the pulsar is on and, by implication, less than average when the pulsar is off. *Panel-B* shows a fit of a simple model with different values of $\dot{\nu}$ for the on and off states to the timing phase residuals [35]

2.5 Pulse Modulation and Drifting

Pulsars exhibit a variety of pulse modulation phenomena which are different to, but never-the-less related to, pulse nulling and mode changing. The power spectrum of pulse-to-pulse fluctuations in pulse energy often shows quasi-periodic components which are usually confined to the outer or conal parts of the pulse profile [2]. Subpulse drifting is a closely related phenomenon in which the pulse phase or longitude of subpulses varies systematically in successive pulses, see for example [63]. The properties of the drifting subpulses, for example, the rate at which they drift across the profile or even their existence, are often affected by nulls and mode changes, illustrating the close connection between these various phenomena [28, 54].

Clear drifting subpulses are only observed in a handful of pulsars. However, a systematic study of 1.4 GHz Westerbork data for 187 pulsars by Weltevrede, Edwards and Stappers [67] has shown evidence for subpulse drifting in 68 pulsars, more than a third of the sample. Taking into account signal/noise limitations, this indicates that more than half of all pulsars have some drifting behaviour. Figure 2.9 illustrates the analysis procedures used. Drifting behaviour is indicated by a concentration of power away from the vertical zero-frequency axis in the 2-dimensional power spectra. Two types of drifting are identified: “coherent” in which the feature

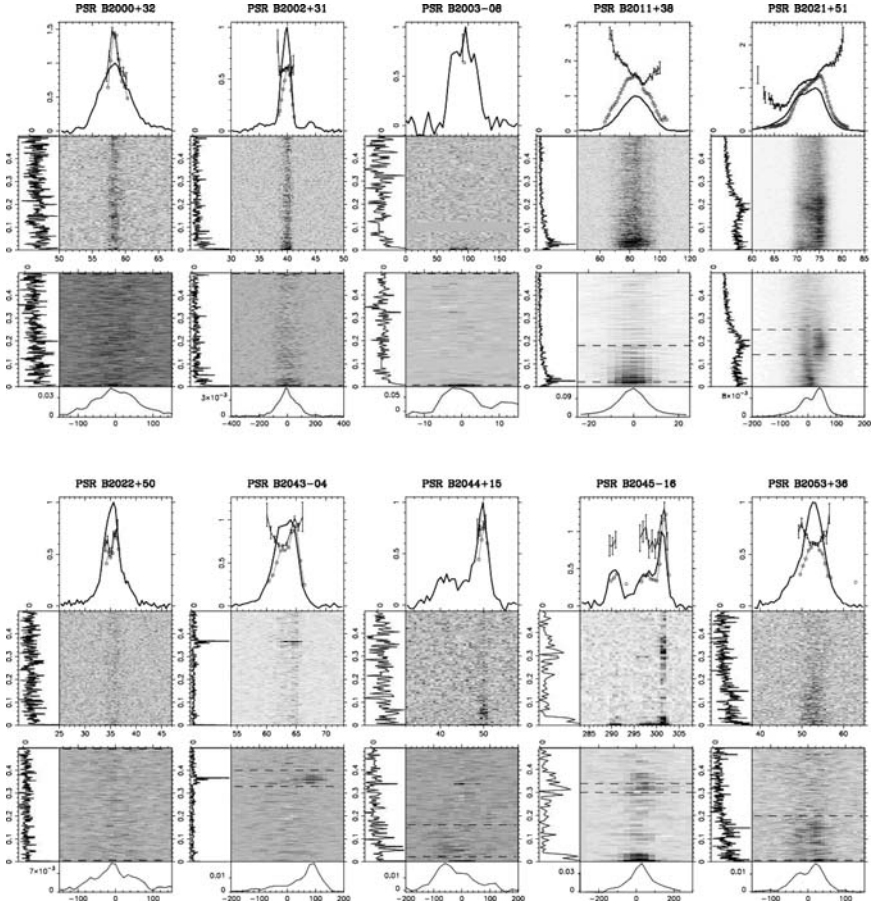

Fig. 2.9 Results of pulse modulation analyses using Westerbork 1.4-GHz data for selected pulsars [67]. In the *upper panel* for each pulsar the mean pulse profile (*solid line*), the variance of the pulse-to-pulse fluctuations (*open circles*) and the corresponding modulation index (points with error bars) are shown as a function of pulse longitude (in degrees). The *middle panels* contain the longitude-resolved fluctuation spectra, i.e., the spectra of time sequences of power in individual longitude bins and the lower panels give the 2-dimensional power spectra of the observed longitude-time variations. The 1-dimensional spectra at the side and bottom are the power integrated across the 2-dimensional plots

in the fluctuation spectrum is narrow (less than 0.05 cycles/period) and "diffuse" in which a wider feature is observed. Examples of the two types given in Fig. 2.9 are PSR B2043−04 (coherent) and PSR B2021+51 (diffuse). Although some pulse modulation indices are larger than 1.0, they are generally smaller, with ∼0.5 being the most common value. There is little correlation of modulation index with the presence or absence of drifting subpulses. However, there is a significant correlation of drifting behaviour with pulsar characteristic age, with older pulsars more likely to show drifting behaviour, especially coherent drifting.

2.6 Giant and Not-So-Giant Pulses

Giant pulses are, by convention, defined to be intense narrow pulses which typically have a pulse energy much greater than that of the average pulse. They are characterized by a power-law distribution of pulse energies and a close association with high-energy (X-ray or γ-ray) pulse emission. They are observed in two classes of pulsars, young energetic pulsars such as the Crab pulsar, which was indeed discovered through its giant pulse emission [58], and MSPs, which also have a high value of spin-down luminosity $\dot{E} = 4\pi^2 I \dot{P} P^{-3}$.

The highest time-resolution observations to date have been published by Hankins et al. [19]. Arecibo observations of the Crab pulsar at 5.5 GHz with a bandwidth of 500 MHz were recorded with a baseband system and coherently de-dispersed to give a maximal time resolution of 2 ns. Figure 2.10 shows that a single giant pulse consists of a series of "nanopulses" with timescales of a few nanoseconds. The extremely short timescale of the nanopulses implies scale sizes for the emitting regions of order 1 m and brightness temperatures of order 10^{37} K. It is likely that these nanopulses are the fundamental units of emission from the coherent process. Their short timescale appears inconsistent with either coherent curvature radiation from electron bunches or maser processes, leaving collapse of wave packets generated by small-scale plasma turbulence as the most likely candidate.

Other recent observations of Crab giant pulses include those of Popov et al. [52] and Jessner et al. [29]. Popov et al. used the Kalyzin 64-m radio telescope at 600 MHz and showed that all pulses in the main pulse and interpulse were giant; i.e., in a long-term synchronous average, the integrated intensity of these two pulse components could be entirely accounted for by the giant pulses. In contrast, no giant

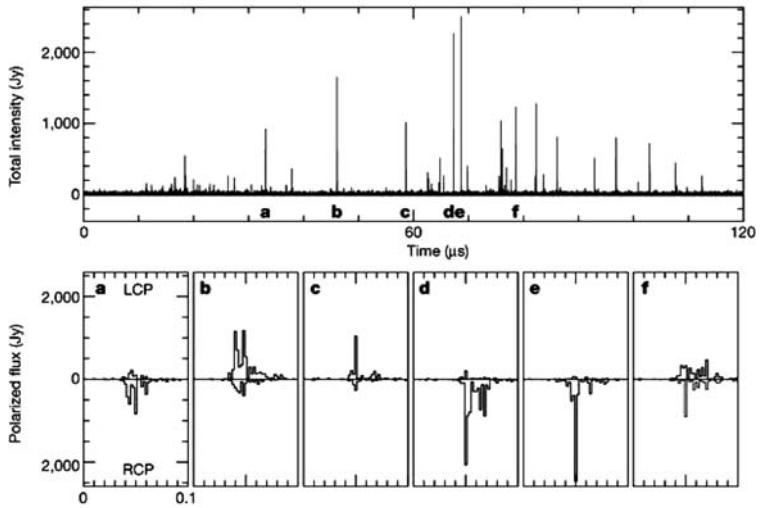

Fig. 2.10 Nanopulses from the Crab pulsar, recorded at 5.5 GHz with the Arecibo radio telescope and coherently de-dispersed to give 2-ns time resolution [19]

pulses were observed from the so-called "precursor" component which precedes the main pulse by about 2 ms, is wider than either the main pulse or the interpulse and is highly linearly polarised.

At high radio frequencies the mean pulse profile has a number of other components which are not seen at lower frequencies (or in X-rays and γ-rays) [48]. Using the Effelsberg 100-m radio telescope at 8.3 GHz, Jessner et al. [29] observed giant pulses, not only from the main pulse and interpulse (at this frequency, the interpulse is much stronger than the main pulse), but also from the two high-frequency components HFC1 and HFC2. A few strong pulses were observed at phases close to the precursor, but it is not clear if they are related to that component.

In the Crab pulsar, the main pulse and interpulse, which as mentioned above are dominated by giant pulses, have precisely the same pulse phase as the peaks of the optical, X-ray and γ-ray pulse components. A similar association of giant pulse emission phases with high-energy pulse components is observed in PSR B1937+21, the original MSP, where both are on the trailing wing of the main radio pulse and interpulse [9]. Recent observations using the 100-m Green Bank telescope at 850 MHz by Knight et al. [31] detected giant pulses from the MSP PSR J0218+4232. As Fig. 2.11 shows, the giant pulses occur at minima in the mean radio

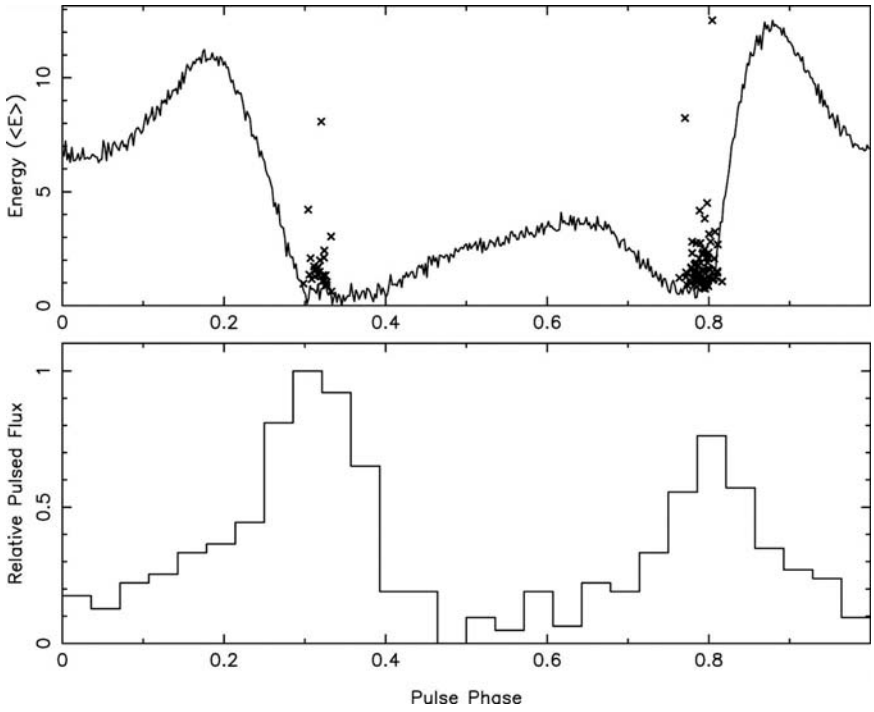

Fig. 2.11 The *top panel* shows the mean pulse profile of PSR J0218+4232 at 850 MHz with the pulse phases and energies of giant pulses marked by crosses. The lower panel shows the *Chandra* 0.1–10 keV X-ray pulse profile phase aligned with the radio profile as emitted from the pulsar (i.e. after correcting for the radio dispersion delay) [31, 36, 55]

profile but are coincident with the phases of the X-ray peaks. These results clearly show that the emission regions for high-energy emission and for giant pulses in both young and millisecond pulsars are closely associated, and that both are distinct from the emission region(s) for the "normal" radio emission.

Very strong individual pulses are observed from more "normal" pulsars. For example, Kuzmin and Ershov [37] observed pulses from PSR B0031−07 at 40 and 111 MHz which were several hundred times as strong as the average pulse. They were confined to a narrower pulse phase range than that covered by the mean pulse profile and were concentrated near the peaks of the mean profile. A very similar phenomenon was observed by Weltevrede et al. [68] at 327 MHz in PSR 0656+14. These results suggest that these are not "giant" pulses in the sense defined at the start of this section. They are much broader, with pulse widths typically several milliseconds, they are related in pulse phase to the normal emission, they do not have a power-law intensity distribution and they are not associated with high-energy emission. Furthermore, these pulsars do not have high values of $\dot{E}$. It seems more likely that these strong pulses reflect extreme examples of normal subpulse modulation. As mentioned in Sect. 2.2 and discussed by Weltevrede et al. [68], it is quite possible that most if not all RRATs are highly modulated pulsars similar to these (but more distant).

2.7 Transient Radio Emission from a Magnetar

Apart from some claimed but unconfirmed detections at low radio frequencies [42, 56], searches for pulsed radio emission from magnetars (AXPs and SGRs) have been unsuccessful. This changed dramatically in March 2006 when strong radio pulses at 1.4 GHz were observed from XTE J1810−197 (PSR J1809−1943) at Parkes [6]. Following a large X-ray flare [24] the AXP was detected as a variable radio continuum source at 1.4 GHz [6, 18]. The Parkes observations revealed strong radio pulses at the 5.54 s period of the AXP which were consistent with the entire radio flux being pulsed. Large day-to-day variations in flux density, which cannot be accounted for by interstellar scintillation, were observed. Observations over a wide range of frequencies using Parkes, the Very Large Array and the Green Bank Telescope showed that, within the uncertainty caused by the flux variations, the pulse spectrum was essentially flat. As Fig. 2.12 shows, strong individual pulses were detected at frequencies as high as 42 GHz, a remarkable and unprecedented result.

This AXP lies within the boundaries of the Parkes Multibeam Pulsar Survey and was observed in 1997 and 1998. No pulsations were detected, showing that the pulsed flux density was less than about 0.2 mJy at that time. This suggests that the strong radio pulsed emission from this object is related to the occurrence of the X-ray flare in early 2003. It is possible that the lack of confirmation of earlier detections of radio emission from magnetars [42, 56] results from a similar transient nature of the pulsed emission.

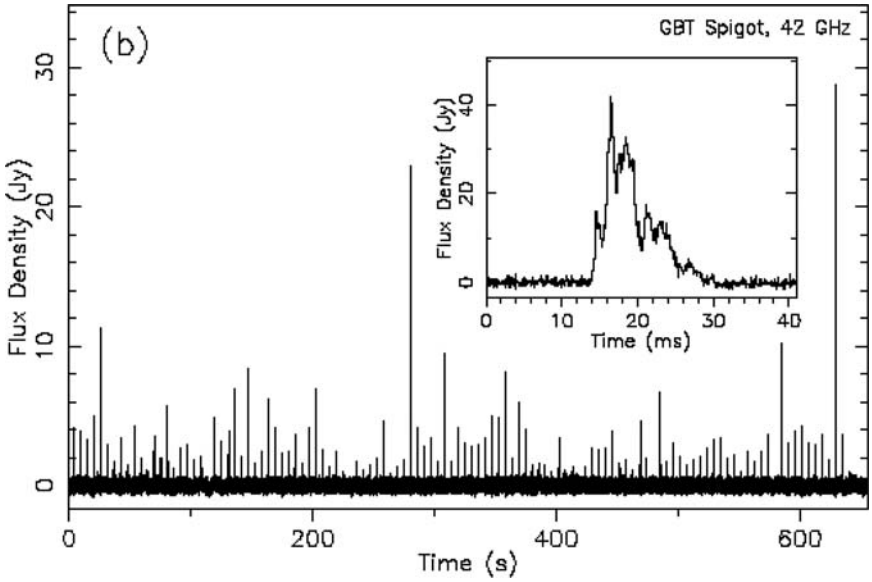

Fig. 2.12 A train of individual pulses from the magnetar PSR J1809−1943 recorded at 42 GHz using the Green Bank Telescope. The inset shows the detailed sub-structure of the strongest pulse recorded with 80 μs resolution [6]

2.8 Rotation Axis: Proper Motion Correlation

The relationship between the direction of the pulsar spin axis and the direction of the pulsar space velocity is important in helping us to understand the origin of pulsar velocities. For example Tademaru and Harrison [61] proposed a "photon rocket" mechanism and, more recently, Spruit and Phinney [57] discussed a "slow kick" model, both of which result in an alignment of the pulsar spin and velocity vectors. Early investigations [1] found no correlation between the projected axis of rotation derived from pulsar polarisation observations and the pulsar proper motion vector, suggesting that the pulsar "rocket" mechanism [61] was not effective in accelerating pulsars. However, many of the pulsars in this sample were relatively old, implying a possible decoupling of the orientation of the current proper motion vector and the spin axis direction because of acceleration in the Galactic gravitational field. Furthermore, the interpretation of the observed position angle variations was complicated by the presence of orthogonal polarisation modes [60]. New light was shed on this by remarkable X-ray results showing equatorial tori surrounding the Crab and Vela pulsars [20, 22, 66]. These tori unambiguously define the orientation of the pulsar spin axis and, in both cases, the direction projected on the sky is close to that of the proper motion [20]. Ng and Romani [51] showed that X-ray tori around several other young pulsars were similarly aligned with their proper motion vectors.

Johnston et al. [30] used Parkes observations to improve rotation measures and fitted the rotating-vector model to the observed position angle (PA) variations to

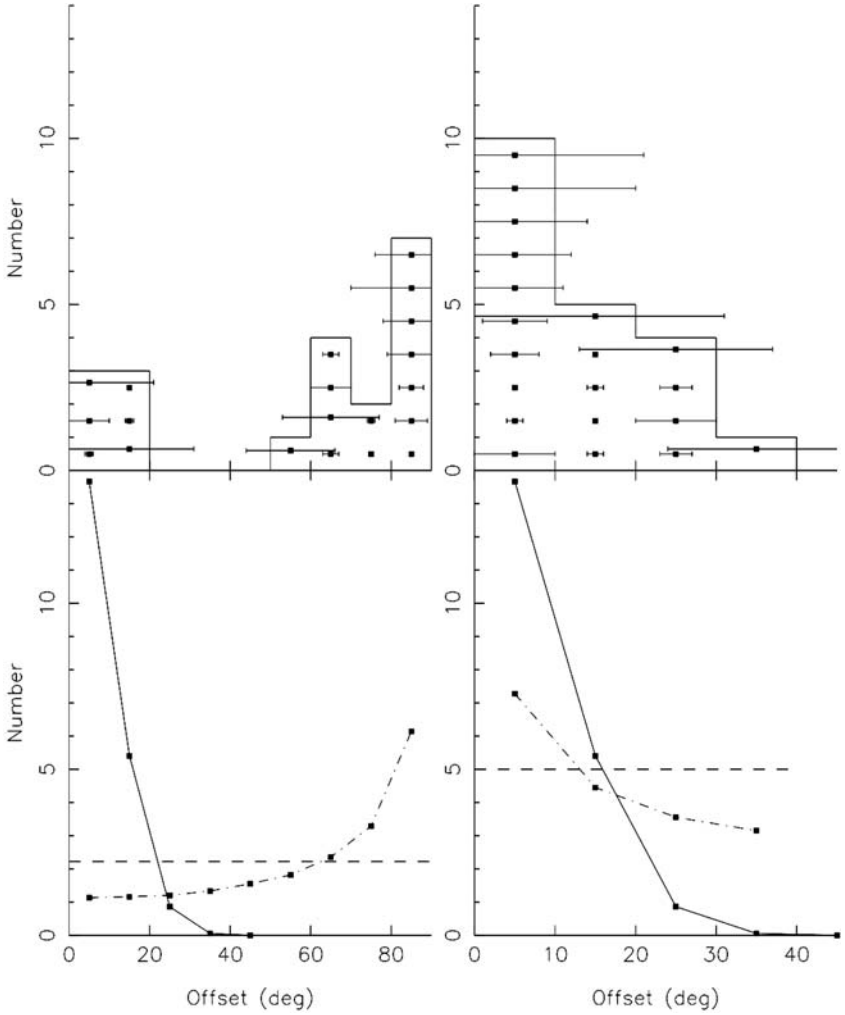

Fig. 2.13 The difference between the position angle of the pulsar rotation axis implied by polarisation observations and the proper motion vector as observed (*top left*) and allowing for the possible presence of orthogonal polarisation modes (*top right*) for 25 pulsars [30]. The *lower panels* show the results of simulations for rotation axes and velocities respectively aligned (*solid line*), orthogonal (*dot-dashed line*) and uncorrelated (*dashed line*)

derive improved estimates of the intrinsic PA of the centre of symmetry of the PA variation across the pulse. The results of comparing these angles with the PA of the proper motion vector are shown in Fig. 2.13. Similar results were obtained by Wang et al. [64] by reanalyzing archival data. Figure 2.13 shows a strong preference for angle differences either close to 0° or to 90° and is inconsistent with a random distribution at the 94% level. If the 90° offsets are attributed to emission in the orthogonal mode (right panel) then the significance improves to 98%. In the case

of three young pulsars, Crab, Vela and PSR B0656+14, this reassignment of the PA difference is confirmed by X-ray and optical observations.

These results strengthen the case for alignment of the rotation and velocity vectors, at least for young pulsars. In the context of the Spruit and Phinney [57] model, they imply that birth kicks effectively act over a time long compared to the birth spin period, so that the components perpendicular to the spin axis average to zero.

2.9 Conclusions

This review has presented a selection, by no means complete, of interesting recent results related to the radio emission from pulsars. Despite the nearly 40 years since their discovery, pulsars remain a highly active and productive field of research. They are distinguished not only by their intrinsic interest, but also by their power and versatility as probes of a wide range of physical and astrophysical problems. Essentially all pulsar observations are sensitivity limited. With new more sensitive facilities such as the Chinese FAST telescope [50] and the Square Kilometer Array [33] being planned, the future of pulsar astronomy is bright.

References

1. Anderson, B. & Lyne, A. G., 1983, Nature, 303, 597
2. Backer, D. C., 1973, ApJ, 182, 245
3. Bhattacharya, D. & van den Heuvel, E. P. J., 1991, Phys. Rep., 203, 1
4. Burgay, M., D'Amico, N., Possenti, A., et al., 2003, Nature, 426, 531
5. Burgay, M., Joshi, B. C., D'Amico, N., et al., 2006, MNRAS, 368, 283
6. Camilo, F., Ransom, S. M., Halpern, J. P., et al., 2006, Nature, 442, 892
7. Cordes, J. M., Freire, P. C. C., Lorimer, D. R., et al., 2006, ApJ, 637, 446
8. Cordes, J. M. & Lazio, T. J. W., 2002, astro-ph/0207156
9. Cusumano, G., Hermsen, W., Kramer, M., et al., 2003, A&A, 410, L9
10. Davies, M. B. & Hansen, B. M. S., 1998, MNRAS, 301, 15
11. Duncan, R. C. & Thompson, C., 1992, ApJ, 392, L9
12. Durdin, J. M., Large, M. I., Little, A. G., et al., 1979, MNRAS, 186, 39P
13. Edwards, R. T., Bailes, M., van Straten, W., et al., 2001, MNRAS, 326, 358
14. Esamdin, A., Lyne, A. G., Graham-Smith, F., et al., 2005, MNRAS, 356, 59
15. Faucher-Giguère, C.-A. & Kaspi, V. M., 2006, ApJ, 643,332
16. Faulkner, A. J., Stairs, I. H., Kramer, M., et al., 2004, MNRAS, 355, 147
17. Goldreich, P. & Julian, W. H., 1969, ApJ, 157, 869
18. Halpern, J. P., Gotthelf, E. V., Becker, R. H., et al., 2005, ApJ, 632, L29
19. Hankins, T. H., Kern, J. S., Weatherall, J. C., et al., 2003, Nature, 422, 141
20. Helfand, D. J., Gotthelf, E. V., & Halpern, J. P., 2001, ApJ, 556, 380
21. Hessels, J. W. T., Ransom, S. M., Stairs, I. H., et al., 2006, Science, 311, 1901
22. Hester, J. J., Scowen, P. A., Sankrit, R., et al., 1995, ApJ, 448, 240
23. Hobbs, G., Faulkner, A., Stairs, I. H., et al., 2004, MNRAS, 352, 1439
24. Ibrahim, A. I., Markwardt, C. B., Swank, J. H., et al., 2004, ApJ, 609, L21
25. Jacoby, B. A., 2004, PhD thesis, Calfornia Institute of Technology
26. Jacoby, B. A., Bailes, M., van Kerkwijk, M. H., et al., 2003, ApJ, 599, L99

27. Jacoby, B. A., Hotan, A., Bailes, M., et al., 2005, ApJ, 629, L113
28. Janssen, G. H. & van Leeuwen, J., 2004, A&A, 425, 255
29. Jessner, A., Słowikowska, A., Klein, B., et al., 2005, Adv. Space Res., 35, 1166
30. Johnston, S., Hobbs, G., Vigeland, S., et al., 2005, MNRAS, 364, 1397
31. Knight, H. S., Bailes, M., Manchester, R. N., et al., 2006, ApJ, 640, 941
32. Kolonko, M., Gil, J., & Maciesiak, K., 2004, A&A, 428, 943
33. Kramer, M., Backer, D. C., Cordes, J. M., et al., 2004, New Astron. Rev., 48, 993
34. Kramer, M., Bell, J. F., Manchester, R. N., et al., 2003, MNRAS, 342, 1299
35. Kramer, M., Lyne, A. G., O'Brien, J. T., et al., 2006, Science, 312, 549
36. Kuiper, L., Hermsen, W., & Stappers, B., 2004, Adv. Space Res., 33, 507
37. Kuzmin, A. D. & Ershov, A. A., 2004, A&A, 427, 575
38. Lorimer, D. R., Faulkner, A. J., Lyne, A. G., et al., 2006, MNRAS, 372, 777
39. Lorimer, D. R., Stairs, I. H., Freire, P. C., et al., 2006, ApJ, 640, 428
40. Lyne, A. G., Burgay, M., Kramer, M., et al., 2004, Science, 303, 1153
41. Lyne, A. G., Manchester, R. N., & Taylor, J. H., 1985, MNRAS, 213, 613
42. Malofeev, V. M., Malov, O. I., & Teplykh, D. A., 2006, Chin. J. Astron. Astrophys., Suppl. 2, 6, 68
43. Manchester, R. N., Fan, G., Lyne, A. G., et al., 2006, ApJ, 649, 235
44. Manchester, R. N., Hobbs, G. B., Teoh, A., et al., 2005, AJ, 129, 1993
45. Manchester, R. N., Lyne, A. G., Camilo, F., et al., 2001, MNRAS, 328, 17
46. McLaughlin, M. A., Lyne, A. G., Lorimer, D. R., et al., 2006, Nature, 439, 817
47. Mdzinarishvili, T. G. & Melikidze, G. I., 2004, A&A, 425, 1009
48. Moffett, D. A. & Hankins, T. H., 1996, ApJ, 468, 779
49. Morris, D. J., Hobbs, G., Lyne, A. G., et al., 2002, MNRAS, 335, 275
50. Nan, R.-D., Wang, Q.-M., Zhu, L.-C., et al., 2006, Chin. J. Astron. Astrophys., Suppl. 2, 6, 304
51. Ng, C.-Y. & Romani, R. W., 2004, ApJ, 601, 479
52. Popov, M., Soglasnov, V., Kondrat'ev, V., et al., 2006, Astron. Lett., 50, 55
53. Ransom, S. M., Hessels, J. W. T., Stairs, I. H., et al., 2005, Science, 307, 892
54. Redman, S. L., Wright, G. A. E., & Rankin, J. M., 2005, MNRAS, 357, 859
55. Rutledge, R. E., Fox, D. W., Kulkarni, S. R., et al., 2004, ApJ, 613, 522
56. Shitov, Y. P., Pugachev, V. D., & Kutuzov, S. M., 2000, In: Pulsar astronomy – 2000 and beyond, IAU Colloquium 177, ed. M. Kramer, N. Wex, & R. Wielebinski (San Francisco: Astronomical Society of the Pacific), 685
57. Spruit, H. & Phinney, E. S., 1998, Nature, 393, 139
58. Staelin, D. H. & Reifenstein, III, E. C., 1968, Science, 162, 1481
59. Staveley-Smith, L., Wilson, W. E., Bird, T. S., et al., 1996, PASA, 13, 243
60. Stinebring, D. R., Cordes, J. M., Rankin, J. M., et al., 1984, ApJS, 55, 247
61. Tademaru, E. & Harrison, E. R., 1975, Nature, 254, 676
62. Tauris, T. M. & Manchester, R. N., 1998, MNRAS, 298, 625
63. Taylor, J. H., Manchester, R. N., & Huguenin, G. R., 1975, ApJ, 195, 513
64. Wang, C., Lai, D., & Han, J. L., 2006, ApJ, 639, 1007
65. Wang, N., Manchester, R. N., & Johnston, S., 2007, MNRAS, 1383
66. Weisskopf, M. C., Hester, J. J., Tennant, A. F., et al., 2000, ApJ, 536, L81
67. Weltevrede, P., Edwards, R. T., & Stappers, B. W., 2006, A&A, 445, 243
68. Weltevrede, P., Stappers, B. W., Rankin, J. M., et al., 2006, ApJ, 645, L149

http://www.springer.com/978-3-540-76964-4

Neutron Stars and Pulsars
Becker, W. (Ed.)
2009, XV, 697 p., Hardcover
ISBN: 978-3-540-76964-4